V International Conference on Simulation for Additive Manufacturing
Sim-AM 2025
F. Auricchio, M. Carraturo and S. Morganti (Eds)

AUTOMATISED OPTIMISATION OF MATERIAL JOINTS FOR ADDITIVE MANUFACTURED MULTIMATERIAL COMPONENTS

CHRISTOPH LEUPOLD*, MAREN PETERSEN*

*University of Bremen, Institute Technology and Education;
Am Fallturm 1, 28359 Bremen, Germany

Key words: multimaterial additive manufacturing (MMAM), fused deposition modeling, voxel-based simulation, interlocking elements, recycling-friendly design

Abstract. The increasing use of multimaterial additive manufacturing (MMAM) offers the opportunity to open further fields of application, such as the production of additively manufactured sensors. However, alongside the opportunities of MMAM, this also poses challenges. One of these challenges is ensuring a sufficiently strong material bond at the joints. This paper describes the development of a method to automatically optimise the material distribution in joints of parts manufactured via the fused deposition modeling process according to the component requirements and the materials used. The method presented is created by coupling different operations:
The main aspect of this approach is the adjustment of a Python-based FEM simulation. The material model assumes transversely isotropic behavior characteristic of fused deposition modeled components, validated in previous studies. To accelerate the calculation of the individual components, a voxel-based approach is used, which has already been successfully applied to similar problems.
For the method, a three-dimensional arrangement of voxels is designed, to each of which one of the materials used can be assigned. In turn, regions are defined between the respective voxels, to which threshold values regarding component failure from experimental tests are assigned. In a series of simulation runs with increasing loads, regions are identified in which damage occurs at the micro level. This damage is modelled using the widely applied approach of local stiffness reduction. If a macro failure is detected due to the formation of a cluster of damaged regions, the simulation runs are stopped. The load used in the penultimate simulation is then used as fitness value for optimising the material assignment to the voxels using a genetic algorithm. Initial tensile tests carried out to evaluate the method show that the tensile strength can be influenced effectively through the use of interlocking elements.

1 MOTIVATION & OBJECTIVE

The possibilities created by technical innovations are expanding the functionalities of additive manufactured components. One advancement introduced in an increasing number of additive processes is the integration of multiple materials within a single component. Multimaterial additive manufacturing (MMAM) enables a wide range of functional possibilities. For example, flexible components can be incorporated into otherwise rigid components, or electrically conductive conductor tracks can be integrated directly as strain sensors [1]. However, these advantages are accompanied by new challenges in the use

of MMAM: For many material combinations, the transition zone represents a mechanical weak point due to poor chemical compatibility [2]. In addition, MMAM components are more difficult to recycle than single-material parts, since efficient recycling requires material purity [3].

An adapted design of MMAM joints can offer a solution to both of these challenges: The use of interlocking elements can increase the joint strength of the connection, even if the chemical compatibility of the material combination is low. For recycling purposes, the joint geometry can be designed such that the interlocking elements contribute primarily act along the main load directions. In less critical directions, their number can be reduced to create predetermined breaking points that facilitate material separation during recycling. This would in turn simplify the material recycling of the individual fragments, as they consist of a high percentage of a uniform material. However, a design that meets both of these objectives is highly dependent on the materials involved, their chemical compatibility, the manufacturing process, the available design space and the expected loads on the component. This makes manual design of the joint complex.

The aim of this study is to develop a method for the automatic design of material transitions that takes these individual boundary conditions into account and enables strong joints even when the materials have low chemical compatibility. A further aim is to further develop this method in such a way that it addresses recycling-friendly design of MMAM.

2 STUDIES ON INCREASING THE STRENGTH OF JOINTS THROUGH THE USE OF INTERLOCKING ELEMENTS

A number of additive processes, such as Fused Deposition Modeling (FDM), Material Jetting, Direct Energy Deposition, Stereolithography or Laser Powder Bed Fusion offer the ability to produce MMAM [4, 5]. However, with some material combinations, the creation of a strong bond between materials is a problem with the different processes [4]. This challenge has already been addressed in various studies, as the following overview shows for the FDM process:

Freund et al. identify the chemical adhesion of the materials and the creation of interlocking elements as particularly important and show which properties and process parameters promote the creation of strong joints [6]. Dairaba-yeva et al., Ermolai et al., Ribeiro et al., Lopes et al. and Frascio et al. investigate different shapes of interlocking elements and demonstrate that different geometries of interlocking elements influence the tensile strength of the joint. [7–11]. Marino et al. demonstrate that interlocking elements also contribute significantly to maximising the strength of the joint under compression. [12]. Kuipers et al. develop and evaluate an ‘interlaced topologically interlocking lattice’ for MMAM, which provides interlocking elements in all spatial directions and thus increases the bond strength under tensile load [13].

These studies show that the joint strength of material combinations with low chemical compatibility can be increased by using interlocking elements. However, how the individual material properties and the specified material compatibility influence the optimal design of the interlocking elements has not yet been investigated. Automated design based on material behaviour can therefore facilitate the widespread use of MMAM, even for materials with low chemical compatibility. The possibility of providing a recycling-friendly MMAM design at the same time also opens up a previously unexplored aspect.

3 DEVELOPED METHOD

The method developed can be divided into three different phases. These are the FEA setup, the simulation procedure and the optimisation. The interaction between the phases is shown in Figure 1.

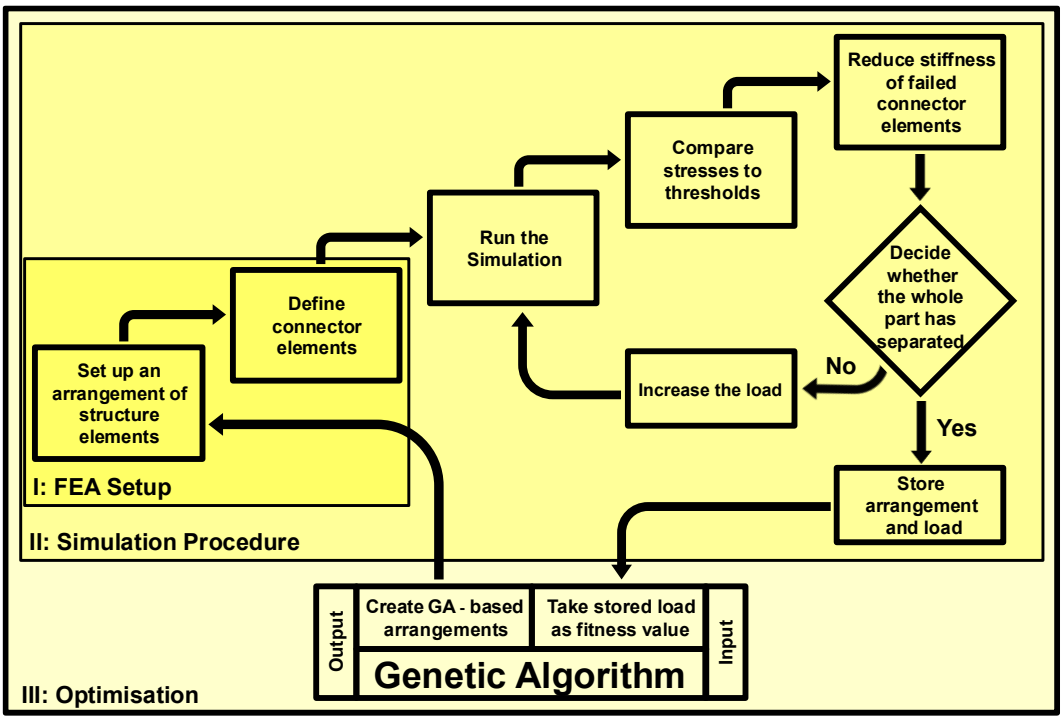

Figure 1: Flow chart of the developed method

I: FEA-Setting:

The FEM package Sfepy [14] is used to perform the simulation, as it offers extensive customisation options and allows direct reuse of simulation results. At the start of the method, the design space for the joint is divided into a spatial arrangement of voxels. The voxel-based approach enables the approximation of any geometry depending on voxel size, allowing the resolution to be adapted to different additive manufacturing processes. Voxel-based optimisation processes are also already used successfully in a wide range of optimisation applications [15]. In the setup used here, the voxels are again divided into two sections. Following the terminology introduced by Woischwill et. al [16], the main part of each voxel is referred to as a structure element, while connector elements cover the space between structure elements. Depending on the location and the materials of the neighbouring structure elements, the connector elements - containing the interface to the next voxel and defining the material transition - can be assigned individual material behaviour (see Figure 2). This option is used to assign experimentally determined threshold values for maximum tensile stress and shear stress to the connector elements.

To represent a connection between the joint and the rest of the component, top and bottom layers are added and completely filled with the respective material. A boundary condition locks the bottom surface of the lowest voxel layer in the Z-direction, while the load is applied to the top surface. The material is modelled as ideally elastic, while the assumption of transverse isotropy follows the findings reported in [17].

II: Simulation Procedure:

The initial tensile load is identical for all arrangements. The stress in each region is calculated, and the average value for each region is determined. For the regions of the connector elements, this average is compared with the respective threshold value. If the average stress exceeds this threshold, failure is simulated by a drastic reduction in stiffness in that region, following the approach described by León-Becerra et al. [18]. Similar to a small rupture in reality, this causes neighbouring structure elements to have almost no mutual interaction at that location. After all regions of the connector elements have been evaluated, the failure of the entire component is assessed. This is done using a pathfinding algorithm that checks whether a continuous path exists between the lowest layer of the simulated area and the top surface without passing through any connector elements with reduced stiffness. If such a path exists, the component remains intact. The simulation then proceeds with an increased load, considering the locally reduced stiffness, and is repeated until the component separates.

III: Optimisation:

A genetic algorithm is employed because the number of possible material arrangements increases exponentially with the number of voxels, making an exhaustive evaluation computationally infeasible even for moderately sized systems. Genetic algorithms are particularly suitable for such discrete optimisation problems, as they efficiently explore large search spaces and can escape local optima through stochastic variation. Furthermore, they allow the simultaneous optimisation of conflicting objectives, such as maximising joint strength in the load direction and minimising it in the recycling direction. In each generation, the algorithm creates populations represented by data matrices that define the material distribution and evaluates them using the maximum load from the simulation that does not cause separation of the arrangement as the fitness value.

4 IMPLEMENTATION AND EXPERIMENTAL VALIDATION

The implementation of the presented method is described in detail in the following, and the initial validation of the results is presented.

4.1 Material properties and manufacturing parameters

Table 1: Manufacturing parameters and sample setup [19]

Manufacturing system	Raise3D Pro3	Schematic set-up and test specimen tensile stress	Schematic set-up and test specimen shear stress
Material 1	PolyLite PLA		
Material 2	PolyLite ABS		
Nozzle size	0.4 mm		
Layer thickness	0.1 mm		
Temperature nozzle 1 (PLA)	225°C		
Temperature nozzle 2 (ABS)	250°C		
Temperature printbed	70°C		
Print velocity (contact surfaces)	20 mm/s		
Print velocity (standard)	30 mm/s		
Infill	100 %		
Pattern:	3 Circular; Inside: 0°/90°		

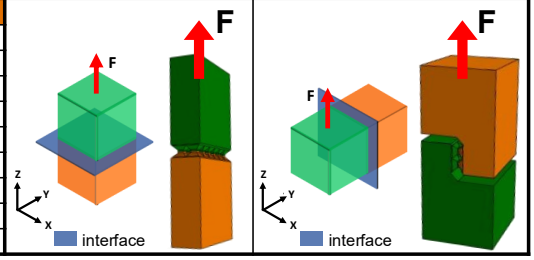

Polylactic Acid (PLA) and Acrylonitrile Butadiene Styrene (ABS) are used to validate the proposed method. The material properties are determined by tensile testing in accordance with DIN ISO 527 on five specimens at a speed of 10 mm per minute using an Inspekt Table 100

testing machine (Hegewald & Peschke) equipped with a 5 kN load cell. The 'ONE' video extensometer (Hegewald & Peschke) was employed together with the testing system to evaluate the Young's modulus and Poisson's ratio All specimens are manufactured with the parameters listed in Table 1. The values for the shear modulus of additive manufactured components made from these materials are taken from the literature [20, 21]. The material properties for the connector elements, which contain both ABS and PLA, are defined by the average value of the two materials. To determine the maximum tensile and shear stresses at which the connector elements fail, test specimens were manufactured and measurements taken in a prior study [19]. All material combinations as well as different build-up and load directions were tested. Schematic structures and the geometry of the test specimens can be seen in Table 1. Table 2 shows the experimentally determined material properties, the index '3' indicates the build direction in the 3D printing process.

Table 2: Material properties used for the simulation

Material	E_1	E_3	v_{12}	v_{13}	G_{13}
PLA	3023 MPa	2619 MPa	0.34	0.27	950 MPa [20]
ABS	2106 MPa	1627 MPa	0.30	0.27	680 MPa [21]
Connector Elements PLA/ABS	2565 MPa	2123 MPa	0.32	0.27	815 MPa

Thresholds tensile stresses[19]				**Thresholds shear stresses** [19]		
PLA on PLA	PLA on ABS	ABS on ABS	ABS on PLA	PLA next to PLA	PLA next to ABS	ABS next to ABS
45.4 MPa	17.9 MPa	19.1 MPa	0 MPa	42.8 MPa	15.2 MPa	17.5 MPa

All other material properties required for the simulation of the behaviour can be determined by assuming transverse isotropy [22].

For transversely isotropic materials, the Poisson's ratios in different directions are interrelated according to

$$\frac{v_{31}}{E_3} = \frac{v_{13}}{E_1} \rightarrow v_{31} = \frac{E_2 * v_{13}}{E_1} \tag{1}$$

The in-plane shear modulus can be calculated from the Young's modulus and the Poisson's ratio using

$$G_{12} = \frac{E_2}{2 * (1 + v_{12})} \tag{2}$$

Since the material is transversely isotropic, the in-plane properties are equal, and the out-of-plane shear moduli are identical. The following relationships therefore hold

$$E_2 = E_1;\ v_{23} = v_{13};\ v_{32} = v_{31};\ G_{23} = G_{13} \tag{3}$$

4.2 Test specimen design

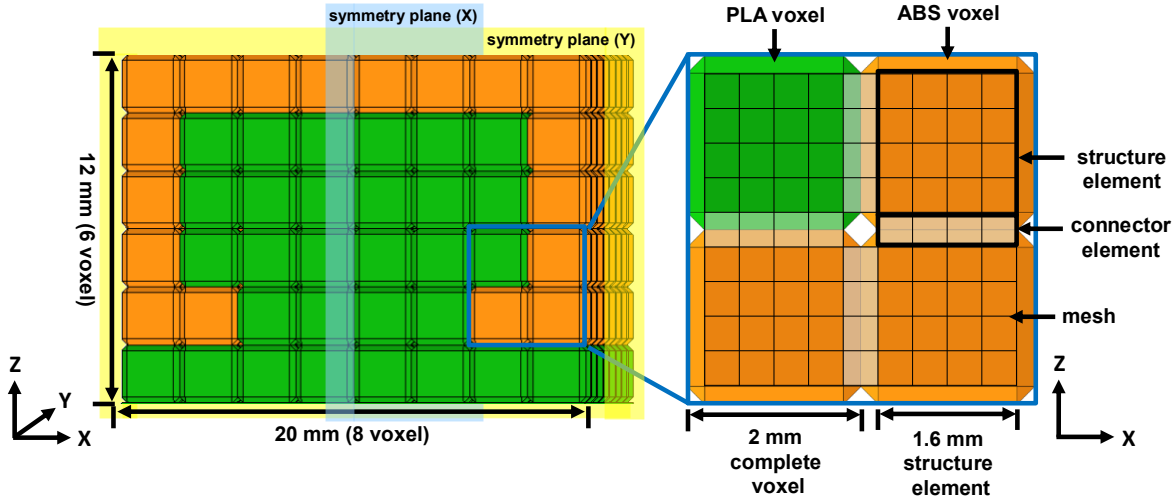

Figure 2: Set-up of the investigated material transition from PLA (bottom) to ABS (top)

To test the method, specimens are prepared according to the following setup. The connection of PLA and ABS with a material transition in the build direction is selected as an example. This combination exhibits low chemical compatibility and limited joint strength [23]. Voxels with an edge length of 2 mm (interfaces 1.6 mm x 1.6 mm) are used to fill a design space of 16 mm × 16 mm × 8 mm (X × Y × Z), applying symmetry in the X and Y directions. This results in a voxel arrangement of 8 × 8 × 6 voxels (X × Y × Z), as a layer of uniform voxels is inserted at the upper and lower boundaries in the Z direction. For the simulation, this corresponds to 96 regions representing the structure elements. Since two structure elements are connected by one connector element, 224 regions are required to represent the entire structure, as shown in Figure 2. In the simulation, these regions are mapped to a Python-generated mesh consisting of 19 × 19 × 29 (X × Y × Z) hexahedral elements. Each structure element comprises 64 mesh elements, and each connector element 16. This setup enables the use of a uniform mesh in which the connector elements are checked for local stiffness reduction. The applied load is increased by 40 N after each run without component separation. Each simulation run takes approximately 60 seconds on a PC with an i7-10875H CPU, 8 GB RTX 2070 GPU, and 16 GB RAM.

4.2 Optimisation

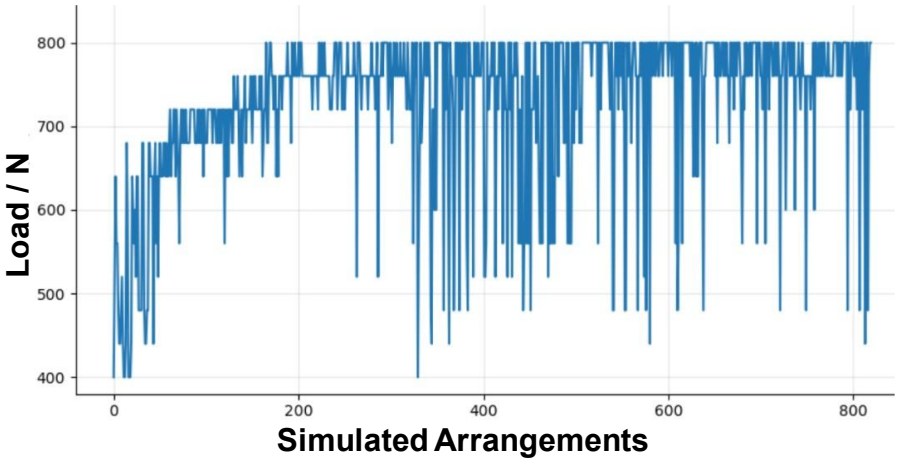

Figure 3: Maximum load for the arrangements created by the genetic algorithm

This setup is coupled with a genetic algorithm, as illustrated in Figure 1. The algorithm generates different material arrangements and uses the maximum load at separation as the fitness value to optimise the design. A crossover probability of 0.7 is chosen to ensure efficient information exchange between promising arrangements while maintaining diversity within the population. The mutation probability per gene is set to 0.4 to introduce sufficient variability and prevent premature convergence, which is particularly important given the discrete and highly non-linear search space. Each generation retains the three best arrangements (elitism) to preserve high-quality solutions, while three random arrangements are introduced every five generations to maintain genetic diversity and avoid local optima. A population size of 20 individuals and 40 generations are selected as a compromise between optimisation depth and computational cost. To further reduce the total optimisation time, a starting load of 400 N is applied for each arrangement.

Figure 3 shows the results for the 800 arrangements created. The optimisation required approximately 25 hours of computation. The results indicate that the maximum value is reached after roughly one quarter of the total runtime, suggesting potential for early-stopping strategies in future studies.

4.3 Validation

To validate the simulation results for manually designed and automatically optimised material arrangements through experiments, a variety of arrangements are designed and tested. Figure 4 shows one example of each of these different arrangements. In addition to the butt joint arrangement (No. 1; black frame), two arrangements with manually designed interlocking elements (No. 2 and No. 3; blue frame) are used. Two arrangements from previous approaches to optimising joint strength are also used for testing (No. 4 and No. 5; red frame). The final arrangement used is one of the arrangements from the optimisation process that showed the highest force (800 N) to separate in the simulation. This sample is shown in Figure 4 (No. 6; gray frame). Three specimens of each of these arrangements are manufactured with the parameter settings listed in Table 1., with each voxel being extruded using the same extruder travel path. A 30 mm long block of solid material is added to the lower and upper ends of the joint to clamp the specimens into the tensile testing machine.

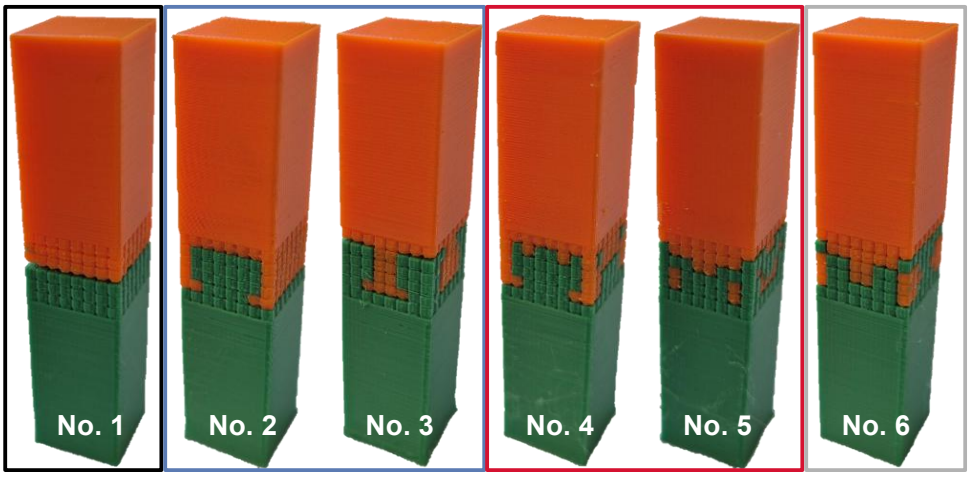

Figure 4: Samples for experimental validation: No. 1 butt joint; No. 2 and No. 3 manually designed, No. 4 and No. 5 from previous optimisation approaches; No. 6 from the proposed approach

The loads determined by simulation and tensile testing are shown in Figure 7. For arrangement No. 1, the simulation shows a separation of the sample under the first load. This value is 40 N, corresponding to the selected step size for increasing the load per run. In the experiment, too, the samples fail under low loads (10–20 N). The manually designed arrangements separate in the simulation at 560 N (No. 2) and 680 N (No. 3) respectively. In the experimental testing, loads between 546 N and 697 N (No. 2) and between 570 N and 585 N (No. 3) were obtained. The values thus vary to very different degrees: while the difference between two individual samples is greatest in arrangement No. 2 at approx. 150 N, arrangement No. 3 shows the smallest percentage difference between the maximum values (2.5%). Arrangements No. 4 and No. 5 show a separation of the components in the simulation under very similar loads: No. 4 at 560 N and No. 5 at 600 N. The experimental results show more notable differences: The samples from No. 4 fail between 438 N and 459 N, while the samples from No. 5 fail at average tensile forces between 552 N and 603 N. According to the optimisation results, the simulation of arrangement No. 6 indicates the highest tensile force with a value of 800 N. In the experiments, however, the samples perform with values between 575 N and 621 N. On average, these values are only slightly above the second-best result (No. 2). Overall, the tensile strength of the optimised joint is thus on a similar level to that of the manually designed joints. As expected, the blunt material transition falls far short of the other solutions. The deviations of the individual samples vary to different degrees. The reasons for the partially large deviations (e.g. No. 2 minimum value: 546 N; maximum value: 697 N) with identical designs have not yet been investigated.

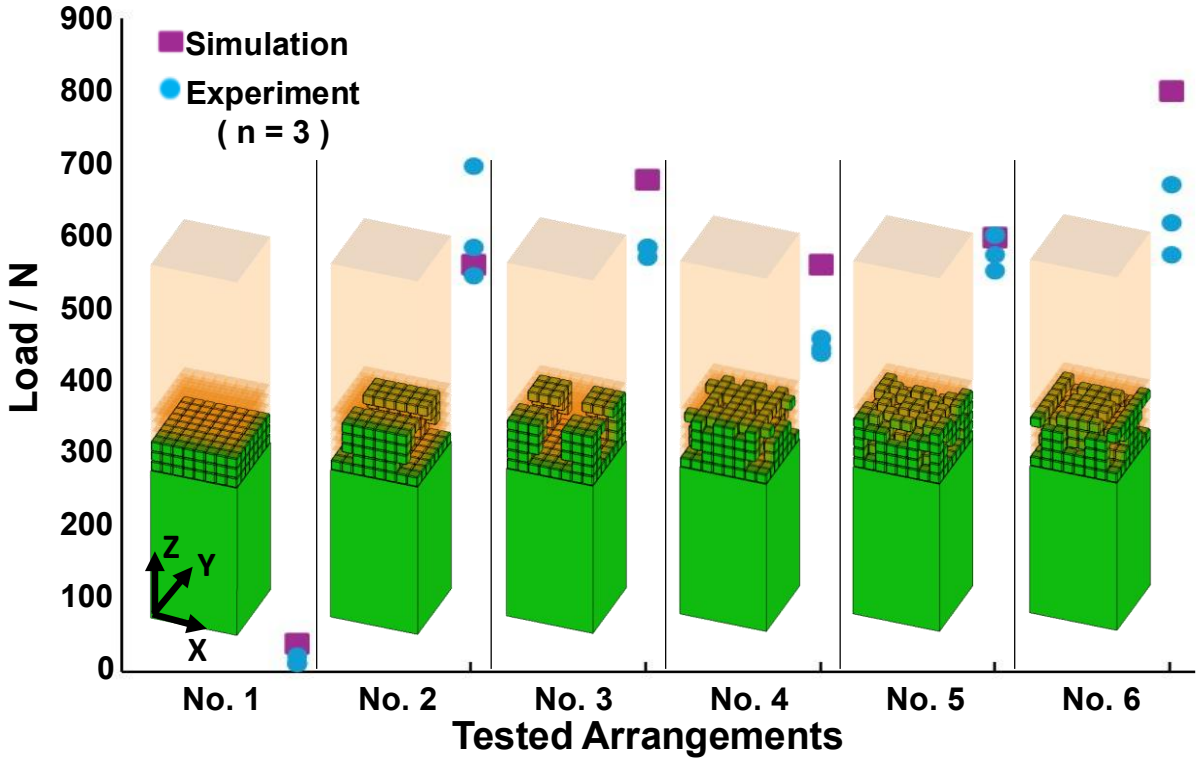

Figure 5: Loads required to separate the joints: values from the simulation compared with the 3 samples from the experiments

5 CONCLUSION AND OUTLOOK

This paper presents a method that combines finite element analysis of material transitions with a genetic algorithm to identify optimised designs for multi-material components, accounting for individual material behaviour and interfacial compatibility. The results demonstrate that the optimised arrangement achieves significantly higher strength than conventional butt joints due to the formation of interlocking elements. The resulting strength is comparable to manually designed structures. However, notable discrepancies remain between simulated and experimentally measured strengths, as well as among samples with identical structures. The underlying causes of these deviations require further investigation. Comparative analyses of simulated and experimental fracture surfaces and strain distributions may provide insights for improving the simulation accuracy.

The potential of the proposed method to enable recycling-friendly material transitions has not yet been verified. Further studies are also needed to investigate whether the formation of interlocking elements can be selectively prevented in specific directions. The observed increase in strength along the primary load direction suggests that targeted optimisation could also suppress such effects in a secondary direction. This hypothesis should be validated in future work through systematic optimisation and experimental evaluation.

REFERENCES

[1] Hossain, M.J., Tabatabaei, B.T., Kiki, M., Choi, J.-W.: Additive Manufacturing of Sensors: A Comprehensive Review *Int. J. of Precis. Eng. and Manuf.-Green Tech*. 12(1), 277–300 (2025). https://doi.org/10.1007/s40684-024-00629-5

[2] Yao, X., Moon, S.K., Bi, G., Wei, J.: A multi-material part design framework in additive manufacturing *Int J Adv Manuf Technol* 99(9-12), 2111–2119 (2018). https://doi.org/10.1007/s00170-018-2025-7

[3] Cruz Sanchez, F.A., Boudaoud, H., Camargo, M., Pearce, J.M.: Plastic recycling in additive manufacturing: A systematic literature review and opportunities for the circular economy *Journal of Cleaner Production* 264, 121602 (2020). https://doi.org/10.1016/j.jclepro.2020.121602

[4] Hasanov, S., Alkunte, S., Rajeshirke, M., Gupta, A., Huseynov, O., Fidan, I., Alifui-Segbaya, F., Rennie, A.: Review on Additive Manufacturing of Multi-Material Parts: Progress and Challenges *JMMP* 6(1), 4 (2022). https://doi.org/10.3390/jmmp6010004

[5] Schneck, M., Horn, M., Schmitt, M., Seidel, C., Schlick, G., Reinhart, G.: Review on additive hybrid- and multi-material-manufacturing of metals by powder bed fusion: state of technology and development potential *Prog Addit Manuf* 6(4), 881–894 (2021). https://doi.org/10.1007/s40964-021-00205-2

[6] Freund, R., Watschke, H., Heubach, J., Vietor, T.: Determination of Influencing Factors on Interface Strength of Additively Manufactured Multi-Material Parts by Material Extrusion *Applied Sciences* 9(9), 1782 (2019). https://doi.org/10.3390/app9091782

[7] Frascio, M., Zafferani, A., Monti, M., Avalle, M.: Investigating enhanced interfacial adhesion in multi-material filament 3D printing: a comparative study of t and Mickey Mouse geometries *Prog Addit Manuf* 9(6), 2113–2122 (2024). https://doi.org/10.1007/s40964-024-00570-8

[8] Lopes, L.R., Silva, A.F., Carneiro, O.S.: Multi-material 3D printing: The relevance of materials affinity on the boundary interface performance *Additive Manufacturing* 23, 45–52 (2018). https://doi.org/10.1016/j.addma.2018.06.027

[9] Dairabayeva, D., Perveen, A., Talamona, D.: Investigation on the mechanical performance of mono-material vs multi-material interface geometries using fused filament fabrication *RPJ* 29(11), 40–52 (2023). https://doi.org/10.1108/RPJ-07-2022-0221

[10] Ermolai, V., Sover, A., Boca, M.A., Hriţuc, A., Slătineanu, L., Nagîţ, G., Stavarache, R.C.: Mechanical Behaviour of Macroscopic Interfaces for 3D Printed Multi-material Samples *MATEC Web Conf.* 368, 1004 (2022). https://doi.org/10.1051/matecconf/202236801004

[11] Ribeiro, M., Sousa Carneiro, O., Da Ferreira Silva, A.: Interface geometries in 3D multi-material prints by fused filament fabrication *RPJ* 25(1), 38–46 (2019). https://doi.org/10.1108/RPJ-05-2017-0107

[12] Peralta Marino, G., La Pierre, S. de, Salvo, M., Díaz Lantada, A., Ferraris, M.: Modelling, additive layer manufacturing and testing of interlocking structures for joined components *Scientific reports* 12(1), 2526 (2022). https://doi.org/10.1038/s41598-022-06521-z

[13] Kuipers, T., Su, R., Wu, J., Wang, C.C.: ITIL: Interlaced Topologically Interlocking Lattice for continuous dual-material extrusion *Additive Manufacturing* 50, 102495 (2022). https://doi.org/10.1016/j.addma.2021.102495

[14] Cimrman, R., Lukeš, V., Rohan, E.: Multiscale finite element calculations in Python using SfePy *Adv Comput Math* 45(4), 1897–1921 (2019). https://doi.org/10.1007/s10444-019-09666-0

[15] Bacciaglia, A., Ceruti, A., Liverani, A.: A systematic review of voxelization method in additive manufacturing *Mechanics & Industry* 20(6), 630 (2019). https://doi.org/10.1051/meca/2019058
[16] Woischwill, C., Kim, I.Y.: Multimaterial multijoint topology *optimization Numerical Meth Engineering* 115(13), 1552–1579 (2018). https://doi.org/10.1002/nme.5908
[17] Zhao, Y., Chen, Y., Zhou, Y.: Novel mechanical models of tensile strength and elastic property of FDM AM PLA materials: Experimental and theoretical analyses *Materials & Design* 181, 108089 (2019). https://doi.org/10.1016/j.matdes.2019.108089
[18] León-Becerra, J., Hidalgo-Salazar, M.Á., González-Estrada, O.A.: Progressive damage analysis of carbon fiber-reinforced additive manufacturing composites *Int J Adv Manuf Technol* 126(5-6), 2617–2631 (2023). https://doi.org/10.1007/s00170-023-11256-w
[19] Leupold, C., Petersen, M.: Approach to an Automated Method for Load-Optimized Design of Multimaterial Joints for Additive Manufacturing. In: Klahn, C., Meboldt, M., Ferchow, J. (eds) *Industrializing Additive Manufacturing*. Springer Tracts in Additive Manufacturing, pp. 115–129. Springer International Publishing, Cham (2024)
[20] Cantrell, J., Rohde, S., Damiani, D., Gurnani, R., DiSandro, L., Anton, J., Young, A., Jerez, A., Steinbach, D., Kroese, C., Ifju, P.: Experimental Characterization of the Mechanical Properties of 3D Printed ABS and Polycarbonate Parts. In: Yoshida, S., Lamberti, L., Sciammarella, C. (eds) *Advancement of Optical Methods in Experimental Mechanics*, Volume 3, pp. 89–105. River Publishers, New York (2025)
[21] Gonabadi, H., Yadav, A., Bull, S.J.: The effect of processing parameters on the mechanical characteristics of PLA produced by a 3D FFF printer *Int J Adv Manuf Technol* 111(3-4), 695–709 (2020). https://doi.org/10.1007/s00170-020-06138-4
[22] Nasdala, L.: FEM-Formelsammlung Statik und Dynamik. *Springer Fachmedien* Wiesbaden, Wiesbaden (2015)
[23] Dağlı, S.: Mechanical Characterization and Interface Evaluation of Multi-Material Composites Manufactured by Hybrid Fused Deposition Modeling (HFDM) *Polymers* 17(12) (2025). https://doi.org/10.3390/polym17121631